

Reflectance difference spectroscopy of gallium phosphide(001) surfaces

D. C. Law, Y. Sun, and R. F. Hicks^{a)}

Department of Chemical Engineering, University of California, Los Angeles, Los Angeles, California 90095.

(Received 16 May 2003; accepted 11 August 2003)

Gallium phosphide(001) surfaces have been prepared by metalorganic vapor-phase epitaxy, and characterized *in situ* by low-energy electron diffraction, x-ray photoemission spectroscopy, and reflectance difference spectroscopy. Three stable phases were observed: (2×1) , (1×1) , and (2×4) with phosphorus coverages of 1.00, 0.67, and 0.13 ML, respectively. Reflectance difference spectra obtained at coverages intermediate between these three values were found to be linear combinations of the spectra of the pure phases. In particular, $\Delta R/R_{(\text{mixed})} = m\Delta R/R_{(1 \times 1)} + (1 - m)\Delta R/R_{(2 \times 1) \text{ or } (2 \times 4)}$, where m is a weighting factor. The weighting factors were used to estimate the phosphorus coverage, and these results agreed to within 5.0% of the values measured by x-ray photoelectron spectroscopy. © 2003 American Institute of Physics.
[DOI: 10.1063/1.1615699]

INTRODUCTION

Gallium phosphide and related compounds are important semiconductor materials that are used in a variety of optoelectronic devices.^{1,2} These devices consist of lattice-matched thin films that are deposited on GaP substrates by metalorganic vapor-phase epitaxy (MOVPE).³ In this process, the precursor molecules, e.g., trimethylgallium and phosphine, adsorb onto the hot crystal surface, decompose, and incorporate the Ga and P atoms into the film. The surface structure of the film can play an important role in MOVPE by affecting the rates of decomposition of the precursor, dopant, and impurity molecules. Therefore, it is useful to understand the stable reconstructions that occur on GaP in the growth environment.

Recent studies of GaP(001) have identified two reconstructions, the (2×1) and (2×4) .^{4–8} These same structures have been observed on InP(001).^{9–12} In particular, scanning tunneling micrographs of the (2×1) reveal that this surface is terminated with rows of buckled P–P dimers, yielding a phosphorus coverage (θ_p) equal to 1.0 ML. Conversely, the (2×4) is composed of rows of Ga–P heterodimers bonded to Ga–Ga dimers in the second layer. In this case, the phosphorus coverage equals 0.13 ML. Two studies of gallium phosphide(001) have noted the presence of a disordered surface intermediate in composition between the (2×1) and (2×4) .^{5,13} However, it was not determined if this surface constitutes a stable phase.

Reflectance difference spectroscopy (RDS) is a useful tool for real-time monitoring of compound semiconductor surfaces.^{4–8,14–23} The optical spectra contain a series of bands arising from the orthogonal arrangements of group-III and group-V dimer bonds, thus making this technique sensitive to the elemental composition of the surface.^{4,8,22,23} Reflectance difference (RD) spectroscopy has been extended to the study of surface reaction kinetics, whereby the signal intensity at a specific energy has been used as a measure of

the group-V coverage.^{16,17,19} Nevertheless, in making these measurements, it is essential to benchmark the RD spectra against other surface characterization tools, such as scanning tunneling microscopy and x-ray photoemission spectroscopy. This benchmarking has been performed for GaAs and InP(001).^{14,15} By contrast, for gallium phosphide(001), the relationship between the RD spectra and the phosphorus coverage has not been determined.

In this article, we report on the phase diagram of GaP(001) prepared by metalorganic vapor-phase epitaxy. In addition to the (2×1) and (2×4) , we observe a distinct (1×1) phase with a phosphorus coverage of 0.67 ± 0.04 ML. Reflectance difference spectra have been recorded for each of these reconstructions, as well as for surfaces at intermediate compositions. It has been found that the spectra of the intermediate phases are linear combinations of those of the pure phases. Moreover, the optical signals have been benchmarked against the phosphorus coverage, and then used for real-time monitoring of the phosphorus desorption rate from GaP (001).

EXPERIMENTAL METHODS

Gallium phosphide films, approximately $0.20 \mu\text{m}$ thick, were deposited on nominally flat S-doped GaP(001) substrates in a horizontal MOVPE reactor. The films were grown at 585°C , 1.3×10^{-4} Torr of trimethylgallium, 0.13 Torr of tertiarybutylphosphine (TBP), and 20 Torr of hydrogen. A SAES pure gas hydrogen purifier, PS4-MT3-H, was used to remove any oxygen, nitrogen, or carbon-containing impurities from the H_2 carrier gas. After deposition, the TBP and H_2 flows were maintained until the samples were cooled to 300 and 40°C , respectively. Then, the crystals were immediately transferred into an ultra-high-vacuum system for surface analysis.

The long-range ordering on the GaP(001) surface was characterized by a Princeton Instruments low-energy electron diffractometer (LEED). Reflectance difference spectra were obtained with an Instruments SA J-Y Nisel spectrometer. The

^{a)}Electronic mail: rhicks@ucla.edu

signal recorded by the instrument corresponded to the difference in reflected light along the $[\bar{1}10]$ and $[110]$ crystal axes divided by the average reflectance intensity, $[(R_{[\bar{1}10]} - R_{[110]})/\langle R \rangle]$.²⁰ Base-line drift was subtracted from the spectrum by taking the average of two RD spectra collected with the polarizing axis oriented $+45^\circ$ and -45° relative to the $[\bar{1}10]$ direction. Core level photoemission spectra of the P 2*p* and Ga 2*p* lines were collected at approximately 133.0 and 1117.0 eV using a PHI 3057 x-ray photoelectron spectrometer with aluminum $K\alpha$ x rays.²⁴ All x-ray photoemission spectroscopy (XPS) spectra were taken in small area mode with a 7° acceptance angle and 23.5 eV pass energy. The take-off angle with respect to the surface normal was 25° .

RESULTS

Three stable phases have been found on the GaP(001) surface. Annealing the out-of-reactor sample at 300, 500, or 550 °C for half an hour results in a (2×1) , (1×1) , or (2×4) surface reconstruction, respectively. Annealing under these temperatures for 8 h does not change the long-range ordering. This indicates that each structure is a thermodynamically stable phase. Figure 1 presents the LEED pattern of these surfaces after the sample has been cooled down to 25 °C. The (1×1) unit cell is designated by the dotted line. The pictures were taken at electron energies of 48, 52, and 50 eV, respectively. The sharp spots observed at low energy and the relatively dark backgrounds indicate that each surface is atomically smooth and the reconstruction is confined to the topmost layers.

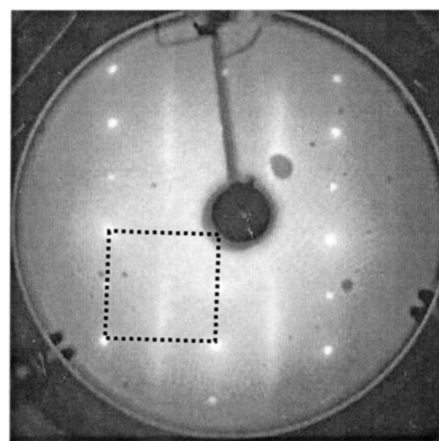
Figure 2 displays the reflectance difference spectra of the (2×1) , (1×1) , and (2×4) structures. The spectrum of the P-rich (2×1) reconstruction contains a series of negative bands between 1.8 and 2.7 eV, and positive peaks at 3.4 and 4.9 eV. The spectrum of the (1×1) exhibits several weak negative bands between 1.8 and 2.5 eV, and two positive peaks at 3.8 and 4.9 eV. On the other hand, the spectrum of the Ga-rich (2×4) contains an intense negative peak at 2.2 eV with a shoulder at 2.5 eV, and positive bands at 3.2, 3.8, and 4.9 eV. The results obtained for the (2×1) and (2×4) phases are in good agreement with previously published RDS data.^{4,5,8}

To determine if the reflectance difference spectra of GaP surfaces intermediate in composition between the (2×1) , (1×1) , and (2×4) are a superposition of the line shapes for these pure phases, the following formulas were applied:

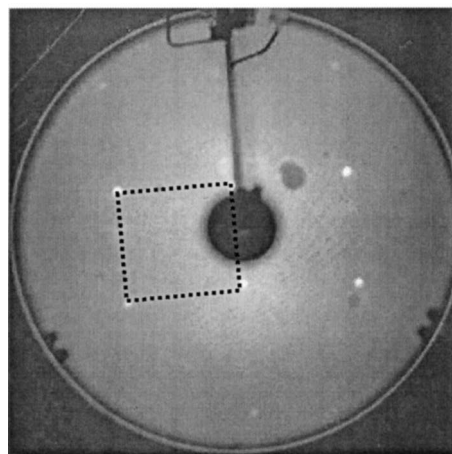
$$\frac{\Delta R}{R}(\text{mixed}) = x \frac{\Delta R}{R}(2 \times 1) + (1-x) \frac{\Delta R}{R}(2 \times 4), \quad (1)$$

$$\frac{\Delta R}{R}(\text{mixed}) = y \frac{\Delta R}{R}(1 \times 1) + (1-y) \frac{\Delta R}{R}(2 \times 1), \quad (2)$$

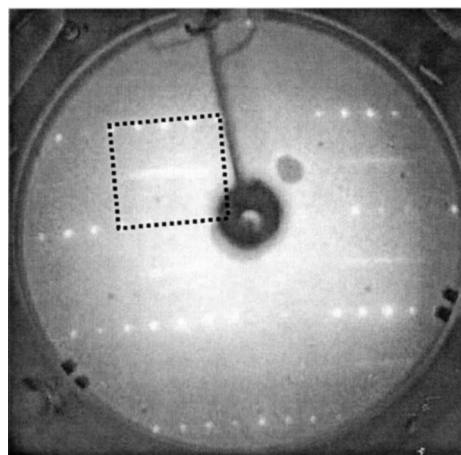
$$\frac{\Delta R}{R}(\text{mixed}) = z \frac{\Delta R}{R}(1 \times 1) + (1-z) \frac{\Delta R}{R}(2 \times 4). \quad (3)$$



(a)



(b)



(c)

FIG. 1. Low-energy electron diffraction patterns of the (a) (2×1) phase, electron energy=48 eV; (b) (1×1) phase, electron energy=52 eV; and (c) (2×4) phase, electron energy=50 eV.

In Eqs. (1), (2), and (3): $\Delta R/R$ (mixed) is the calculated RD spectrum; $\Delta R/R(2 \times 1)$, $\Delta R/R(1 \times 1)$, and $\Delta R/R(2 \times 4)$ are the (2×1) , (1×1) , and (2×4) spectra presented in Fig. 2; and x , y , and z are weighting factors. The weighting factors are the fractional contributions of the (2×1) , (1×1) ,

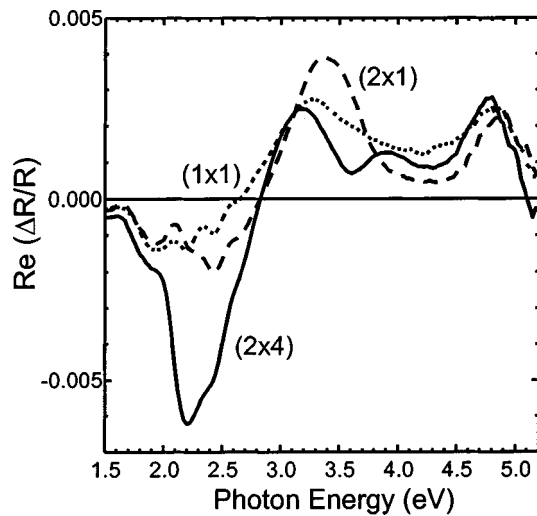


FIG. 2. Reflectance difference spectra of the GaP(001) reconstructions.

and (2×4) line shapes to the overall spectrum. For the GaP (1×1) surface, we are not able to duplicate the optical signal using Eq. (1). The intermediate spectrum is not a combination of the (2×1) and (2×4) spectra. Moreover, Eq. (1) fails to reproduce any observed mixed-phase spectra. In contrast, we have found that the mixed-phase spectra can be replicated with Eqs. (2) and (3), and that they are in excellent agreement with the recorded RDS signals. Examples of these fits are shown in Fig. 3.

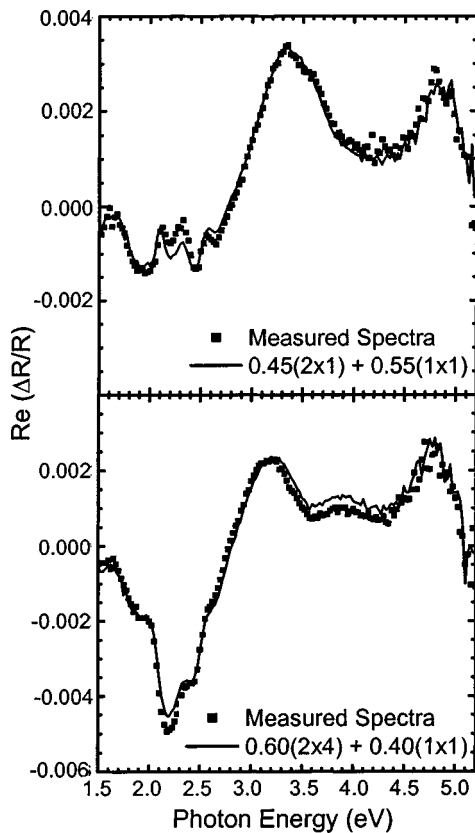


FIG. 3. Comparison of the measured RD spectra to those calculated from Eqs. (2) and (3).

TABLE I. Summary of the LEED, XPS, and RDS measurements of the GaP(001) surfaces.

LEED pattern	P atomic % by XPS	P coverage from XPS data	Weighting factor, y , in Eq. (2).	Weighting factor, z , in Eq. (3).	P coverage from RDS data
(2×1)	42.5	1.00		0.00	1.00
(2×1)	41.3	0.82		0.30	0.90
w(2×1)	41.1	0.78		0.55	0.82
(1×1)	40.6	0.71		0.75	0.75
(1×1)	40.4	0.67	1.00	1.00	0.67
w(2×4)	39.9	0.61	0.80		0.56
(2×4)	38.6	0.42	0.40		0.34
(2×4)	36.7	0.13	0.00		0.13

Annealing (2×1) reconstructed GaP(001) crystals at 550 °C in ultra-high-vacuum results in phosphorus desorption from the surface. By varying the annealing time between 1 and 30 min, every intermediate coverage between the (2×1) and (2×4) phases could be obtained. Listed in Table I are the LEED, XPS, and RDS data recorded for this set of samples. As the LEED pattern changes from (2×1) to (2×4), the atomic concentration of phosphorus measured by XPS falls from 42.5% to 36.7%. These concentrations correspond to the number of P and Ga atoms detected over the photoelectron escape depth, which obviously includes both surface and bulk contributions.^{25,26} Below, a model is presented that relates the phosphorus atomic percentage to the surface coverage.

The photoemission process may be described by the following equation:^{27,28}

$$I_P = \exp\left(\frac{-l}{\lambda_P \cos \alpha}\right), \tag{4}$$

where I_P is the P 2*p* peak intensity for a GaP surface; l is the distance from the surface into the bulk; λ_P is the P 2*p* inelastic mean-free path (i.e., the escape depth), which equals 25 Å;^{29,30} and α is the take-off angle, 25°. Since the photoelectrons are being ejected from a gallium phosphide film, the depth-dependent intensity must be multiplied by the fraction of crystal lattice sites occupied with P atoms. The normalized intensity of the P 2*p* photoemission line is

$$I_{P/GaP} = (2N_P/N_T) \exp\left(\frac{-l}{\lambda_P \cos \alpha}\right), \tag{5}$$

Here, N_T and N_P are the total atom and phosphorus atom concentrations (atoms/cm³), respectively. To calculate the phosphorus atomic percentage, we have:²⁸

$$P(\text{atom \%}) = \frac{\int_0^\infty N_P \exp\left(\frac{-l}{\lambda_P \cos \alpha}\right) dl}{\int_0^\infty N_P \exp\left(\frac{-l}{\lambda_P \cos \alpha}\right) dl + \frac{\lambda_P}{\lambda_{\text{Ga}}} \int_0^\infty N_{\text{Ga}} \exp\left(\frac{-l}{\lambda_{\text{Ga}} \cos \alpha}\right) dl} \quad (6)$$

Here, λ_{Ga} is the Ga 2*p* inelastic mean-free path, which is 12.5 Å.^{29,30} Equation (6) has been solved by summing the expressions inside the integrands over the first 25 atomic layers of the film.

In Eq. (6), N_P is related to θ_P as $\theta_P = N_P / (0.5N_T)$. The effect of coverage on the atomic concentration of phosphorus has been investigated by inserting different values of N_P into Eq. (6), and a linear relationship has been obtained:

$$P(\text{atom \%}) = 6.71\theta_P + 40.33. \quad (7)$$

To examine the accuracy of Eq. (7), one can insert a θ_P of 1.0 or 0.13 for the pure (2×1) or (2×4) phases and compare the result to the XPS measurement. From Eq. (7), the P atom % for these two reconstructions is 47.0 and 41.2, respectively, whereas the XPS data give 42.5 and 36.7 (see column 2, Table I). Evidently, the values from the model are shifted 4.5% higher than those from the experiments. Accordingly, the intercept of Eq. (7) has been decreased by this amount to bring the model in line with the experimental data. With the modified equation, θ_P of the mixed-phase GaP(001) surfaces has been estimated from the XPS data. These results are presented in column 3 of Table I. It is seen that the (1×1) structure exhibits a phosphorus coverage of 0.67 ± 0.04 ML.

The amount of phosphorus on the GaP(001) surfaces may be estimated from the RDS data as well. The phosphorus coverage is obtained from the weighting factors in Eqs. (2) and (3) as follows:

$$\begin{aligned} \theta_P &= y\theta_P(1\times 1) + (1-y)\theta_P(2\times 1) \\ &= 1.0 - 0.33y \quad \text{for } 0.67 < \theta_P < 1.0, \end{aligned} \quad (8)$$

$$\begin{aligned} \theta_P &= z\theta_P(1\times 1) + (1-z)\theta_P(2\times 4) \\ &= 0.13 + 0.54z \quad \text{for } 0.13 < \theta_P < 0.67. \end{aligned} \quad (9)$$

The fractional coverages calculated from Eqs. (8) and (9) are listed in column 6 of Table I. The values of θ_P determined from the RDS results are in good agreement with those determined by XPS. The average percentage difference between the two methods is 5.0%.

DISCUSSION

Three stable phases have been identified on GaP(001), the (2×1), (1×1), and (2×4). Former scanning tunneling microscopy (STM) studies of the (2×1) indicate that it is terminated with one buckled phosphorus dimer per unit cell, similar to the InP(001)-(2×1) reconstruction.^{5,9} According to a recently published article, the (2×1) may be stabilized by 0.5 ML of hydrogen.¹⁰ In this case, the buckled down P atom is bonded to a H atom, while the buckled up P atom contains a lone pair of electrons in its dangling bond. This

structure obeys the electron counting model for compound semiconductor surfaces.³¹ The GaP(001) films examined in this study have been prepared by MOVPE, in which reactive hydrogen is supplied to the surface from the tertiarybutylphosphine source. Consequently, the (2×1) reconstructions may contain 0.5 ML of H atoms adsorbed onto 1.0 ML of P atoms. As for the GaP(001)-(2×4), one may assume that this structure corresponds to the well-accepted heterodimer model.^{11,12} Here, each unit cell contains one Ga-P dimer bonded to four Ga-Ga dimers in the next lower layer, yielding a phosphorus coverage of 0.13 ML.^{5,7,13}

In this work, a GaP(001)-(1×1) reconstruction has been identified by LEED, RDS, and XPS. This structure is intermediate between the (2×1) and (2×4) with a phosphorus coverage of 0.67 ± 0.04 ML. Other researchers have seen evidence for this structure, although they did not verify that it was a distinct phase.^{5,13} We have found that the (1×1) is the only reconstruction present on the GaP(001) surface during extended annealing at 480–540 °C in ultrahigh vacuum. Upon heating the crystal above 540 °C, phosphorus desorbs from the surface causing the (1×1) to smoothly transform into the (2×4).

Shown in Fig. 4 is a proposed ball-and-stick model for the (1×1). It is terminated with phosphorus and gallium dimers in the correct ratio to yield $\theta_P = 0.67$. The dimers are randomly distributed over the surface so that one would observe a (1×1) LEED pattern. Note that every P dangling bond is filled with a pair of electrons, while every Ga dangling bond is empty, thereby satisfying the electron counting model. One may view this surface as originating from a mixture of 33% $\alpha(2\times 4)$ and 67% $\beta(2\times 4)$, in which the arrangements of the dimers are subsequently scrambled.³² In particular, the 2× and ×4 periodicities are lost by individual phosphorus dimers randomly shifting one lattice spacing in the [−110] and [110] directions, respectively.

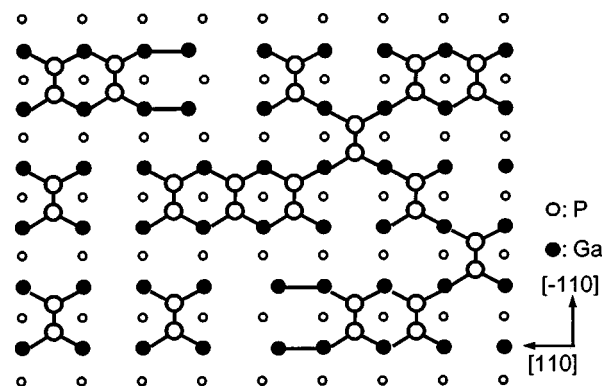


FIG. 4. Ball-and-stick model for a GaP(001) surface containing a random mixture of phosphorus and gallium dimers with $\theta_P = 67\%$.

We have tried to obtain STM micrographs of the (1×1) , but evidently due to the disordered nature of this reconstruction, no atomic resolution images could be obtained. In the study by Fukuda *et al.*, it was shown that when a (2×4) surface is treated with TBP, the dimer rows intermix with each other, creating disordered domains.¹³ If allowed to continue to completion, this would produce a (1×1) structure. Further work should be undertaken to examine low coverages of (1×1) domains contained within predominantly (2×4) or (2×1) phases.

It is interesting to compare the reflectance difference spectra obtained for the (2×1) and (2×4) phases of GaP(001) to those obtained for the same reconstructions on InP(001). The RD spectrum of InP(001)- (2×1) exhibits a sharp positive peak at 3.1 eV that is most likely associated with electronic transitions involving the phosphorus dimer bonds.²³ As can be seen in Fig. 2, a similar positive peak is seen for GaP(001)- (2×1) at 3.4 eV. On the other hand, the RD spectra for GaP(001)- (2×4) shows a broad negative band at 2.2–2.4 eV. This feature is analogous to the negative band seen on InP(001)- (2×4) , except that it is shifted approximately 0.4 eV to higher energies.^{14,17,22,23} Schmidt *et al.*²² have performed first-principles calculations of the optical transitions occurring on the InP (2×4) surface, and have concluded that the negative band arises from transitions between second layer In–In dimers and first layer In–P heterodimers. It seems likely that the negative RDS peaks observed for the GaP (2×4) surface originate from the same transitions between Ga–Ga and Ga–P dimers.

Turning now to the RD spectrum of the GaP(001)- (1×1) phase (c.f., Fig. 2), one sees that the positive peak associated with phosphorus dimers has decreased in intensity relative to the spectrum of the (2×1) . The ratio of the (1×1) peak height to the (2×1) peak height is 0.7. In addition, the intense negative band at 2.2–2.4 eV recorded for the (2×4) is noticeably absent from the optical signature for the (1×1) . These differences in the RDS data are consistent with the model for the (1×1) reconstruction shown in Fig. 4. The ratio of the number of phosphorus dimers on the (1×1) to those on the (2×1) is 0.67, in agreement with the change in height of the 3.4 eV feature. Furthermore, the (1×1) does not contain the heterodimer structure that gives rise to the negative bands near 2.3 eV.

For GaP(001) surfaces at intermediate coverages between the (2×1) , (1×1) , and (2×4) , we have found that reflectance difference spectra are accurately represented by linear combinations of the RD spectra of the pure phases. Surfaces in the range $1.0 > \theta_p > 0.67$ ML obey Eq. (2), in which the (2×1) and (1×1) spectra combine to give the correct optical signature. On the other hand, surfaces with $0.67 > \theta_p > 0.13$ ML obey Eq. (3), in which the (1×1) and (2×4) spectra combine to give the correct spectrum. Reflectance difference spectroscopy of mixed phases of indium phosphide(001) exhibit this same behavior, except that in this case, the optical spectra at intermediate coverages are linear combinations of the RD line shapes for the pure (2×1) and (2×4) phases.¹⁴

Based on the results presented above, RDS may be used for real-time monitoring of the phosphorus coverage on

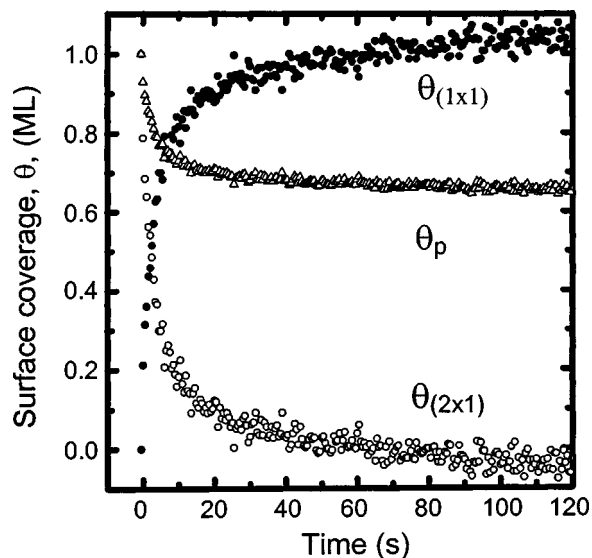


FIG. 5. Dependence of the fractional coverages of the (2×1) and (1×1) phases and of the phosphorus coverage on time during phosphorus desorption from the GaP(001) surface at 550 °C.

GaP(001) during processing. We have found that it is convenient to monitor the signal intensities at 2.3 and 3.4 eV. These signals attain minimum absolute values when the surface is terminated with the (1×1) reconstruction. By recording both signals, one may determine the phase transition to and away from this reconstruction. When the sample is heated to between 500 and 600 °C, the intensities of the RDS peaks decrease slightly and the peak maxima shift somewhat to lower energies.³³ These changes are easily taken into account, so that accurate measurements of the phosphorus coverage may be obtained.¹⁷ An example application of the RDS monitoring technique is presented in the next paragraph.

At temperatures between 480 and 540 °C, we have found that the GaP(001)- (2×1) decomposes into the (1×1) in under 20 min, but that no further phosphorus desorption occurs over 8 h. Consequently, the surface coverage of the (2×4) is zero throughout the experiment. By monitoring the peak intensity at ~ 3.4 eV, the fraction of the (2×1) and (1×1) phases on the surface may be obtained, and then the P coverage calculated from Eq. (8). Presented in Fig. 5 are curves showing the dependence of the fractional coverages of (2×1) , (1×1) , and phosphorus on time during annealing of the GaP(001) crystal at 510 °C in ultrahigh vacuum. At time zero, the phosphine pressure in the chamber was reduced from 1.0×10^{-4} to $< 1.0 \times 10^{-9}$ Torr. Examination of the results presented in Fig. 5 reveals that the phosphorus coverage decays exponentially with time. From these data, the first-order rate constant for phosphorus desorption, k_d , is calculated to be 0.052 s^{-1} . A detailed discussion of the kinetics of phosphine adsorption and phosphorus desorption from gallium phosphide is provided elsewhere.³⁴

CONCLUSIONS

Gallium phosphide(001) surfaces prepared by metalorganic vapor-phase epitaxy have been found to exhibit three stable reconstructions: the (2×1) , (1×1) , and (2×4) with

θ_p equal to 1.00, 0.67, and 0.13 ML, respectively. The (1×1) appears to be terminated with a disordered arrangement of phosphorus and gallium dimers in a 4 to 1 ratio. Reflectance difference spectra of the GaP(001) surfaces have been benchmarked against the XPS data. It was found that the RD line shapes recorded at any coverage can be accurately represented by linear combinations of (2×1) and (1×1), or (1×1) and (2×4) spectra. These results allow one to use RDS for real-time monitoring of the phosphorus coverage during GaP processing.

ACKNOWLEDGMENTS

Funding for this work was provided by the National Science Foundation, UC-SMART, Northrup Grumman (formerly TRW Space and Electronics), Epichem, Inc., and Emcore, Inc.

- ¹F. A. Kish, F. M. Steranka, D. C. DeFevre, D. A. Vanderwater, K. G. Park, C. P. Kuo, T. D. Osentowski, M. J. Peanasky, J. G. Yu, R. M. Fletcher, D. A. Steigerwald, M. G. Craford, and V. M. Robbins, *Appl. Phys. Lett.* **64**, 2839 (1994).
- ²G. E. Hoffer, C. Carter-Coman, M. R. Krames, N. F. Gardner, F. A. Kish, T. S. Tan, B. Loh, J. Posselt, D. Collins, and G. Sasser, *Electron. Lett.* **34**, 1781 (1998).
- ³G. B. Stringfellow, *Organometallic Vapor-Phase Epitaxy: Theory and Practice* (Academic, San Diego, 1989).
- ⁴M. Zorn, B. Junno, T. Trepk, S. Bose, L. Samuelson, J.-T. Zettler, and W. Richter, *Phys. Rev. B* **60**, 11557 (1999).
- ⁵L. Toben, T. Hannappel, K. Moller, H.-J. Crawack, C. Pettenkofer, and F. Willig, *Surf. Sci.* **494**, 755 (2001).
- ⁶N. Esser, W. G. Schmidt, J. Bernholc, A. M. Frisch, P. Vogt, M. Zorn, M. Pristovsek, W. Richter, F. Bechstedt, Th Hannappel, and S. Visbeck, *J. Vac. Sci. Technol. B* **17**, 1691 (1999).
- ⁷K. Lüdge, P. Vogt, O. Pulci, N. Esser, F. Bechstedt, and W. Richter, *Phys. Rev. B* **62**, 11046 (2000).
- ⁸A. M. Frisch, W. G. Schmidt, J. Bernholc, M. Pristovsek, N. Esser, and W. Richter, *Phys. Rev. B* **60**, 2488 (1999).
- ⁹L. Li, B.-K. Han, Q. Fu, and R. F. Hicks, *Phys. Rev. Lett.* **82**, 1879 (1998).
- ¹⁰W. G. Schmidt, P. H. Hahn, F. Bechstedt, N. Esser, P. Vogt, A. Wange, and W. Richter, *Phys. Rev. Lett.* **90**, 126101-1 (2003).
- ¹¹L. Li, Q. Fu, C. H. Li, B.-K. Han, and R. F. Hicks, *Phys. Rev. B* **61**, 10223 (2000).
- ¹²W. G. Schmidt, F. Bechstedt, N. Esser, M. Pristovsek, Ch. Schultz, and W. Richter, *Phys. Rev. B* **57**, 14596 (1998).
- ¹³Y. Fukuda, N. Sekizawa, S. Mochizuka, and N. Sanada, *J. Cryst. Growth* **221**, 26 (2000).
- ¹⁴M. J. Begarney, C. H. Li, C. D. Law, S. B. Visbeck, Y. Sun, and R. F. Hicks, *Appl. Phys. Lett.* **78**, 55 (2001).
- ¹⁵M. J. Begarney, L. Li, C. H. Li, C. D. Law, Q. Fu, and R. F. Hicks, *Phys. Rev. B* **62**, 8092 (2000).
- ¹⁶J. T. Zettler, J. Rumberg, K. Ploska, K. Stahrenberg, M. Pristovsek, W. Richter, M. Wassermeier, P. Schutzenduwe, J. Behrend, and L. Daweritz, *Phys. Status Solidi A* **152**, 35 (1995).
- ¹⁷Y. Sun, S. B. Visbeck, D. C. Law, and R. F. Hicks, *Surf. Sci.* **513**, 256 (2002).
- ¹⁸M. Zorn, P. Kurpas, A. I. Shkrebti, B. Junno, A. Bhattacharya, K. Knorr, M. Weyers, L. Samuelson, J. T. Zettler, and W. Richter, *Phys. Rev. B* **60**, 8185 (1999).
- ¹⁹M. Pristovsek, T. Trepk, M. Klein, J. T. Zettler, and W. Richter, *J. Appl. Phys.* **87**, 1245 (2000).
- ²⁰D. E. Aspnes, J. P. Harbison, A. A. Studna, and L. T. Florez, *Appl. Phys. Lett.* **52**, 957 (1988).
- ²¹H. Tanaka, E. Colas, I. Kamiya, D. E. Aspnes, and R. Bhat, *Appl. Phys. Lett.* **59**, 3443 (1991).
- ²²W. G. Schmidt, N. Esser, A. M. Frisch, P. Vogt, J. Bernholc, F. Bechstedt, M. Zorn, T. Hannappel, S. Visbeck, F. Willig, and W. Richter, *Phys. Rev. B* **61**, R16335 (2000).
- ²³D. C. Law, Q. Fu, S. B. Visbeck, Y. Sun, C. H. Li, and R. F. Hicks, *Surf. Sci.* **496**, 121 (2001).
- ²⁴C. D. Wagner, W. M. Riggs, L. E. Davis, J. F. Moulder, and G. E. Muilenberg, *Handbook of X-Ray Photoelectron Spectroscopy* (Perkin-Elmer, Eden Prairie, MN, 1979).
- ²⁵D. C. Law, Y. Sun, C. H. Li, S. B. Visbeck, G. Chen, and R. F. Hicks, *Phys. Rev. B* **66**, 45314 (2002).
- ²⁶C. H. Li, L. Li, D. C. Law, S. B. Visbeck, and R. F. Hicks, *Phys. Rev. B* **65**, 2053221 (2002).
- ²⁷L. C. Feldman and J. W. Mayer, *Fundamentals of Surface and Thin Film Analysis* (Elsevier Science, New York, 1986).
- ²⁸Y. Feurprier, Ch. Cardinaud, and G. Turban, *J. Vac. Sci. Technol. B* **16**, 1823 (1998).
- ²⁹S. Tanuma, C. J. Powell, and D. R. Penn, *Acta Phys. Pol. A* **81**, 169 (1992).
- ³⁰G. Gergely, M. Menyhard, S. Gurban, Zs. Benedek, Cs. Daroczi, V. Rakovics, J. Toth, D. Varga, M. Krawczyk, and A. Jablonski, *Surf. Interface Anal.* **30**, 195 (2000).
- ³¹M. D. Pashley, *Phys. Rev. B* **40**, 10481 (1989).
- ³²A. Ohtake, M. Ozeki, T. Yasuda, and T. Hanada, *Phys. Rev. B* **65**, 165315 (2002).
- ³³S. B. Visbeck, T. Hannappel, M. Zorn, J.-T. Zettler, and F. Willig, *Phys. Rev. B* **63**, 245 (2001).
- ³⁴Y. Sun, D. C. Law, and R. F. Hicks, *Surf. Sci.* **540**, 12 (2003).